Cement & Concrete Composites 44 (2013) 1–8

Contents lists available at ScienceDirect

Cement & Concrete Composites

journal homepage: www.elsevier.com/locate/cemconcomp

Synthesis, characterization and properties of calcium ferroaluminate belite cements produced with electric arc furnace steel slag as raw material

R.I. Iacobescu [a,b], Y. Pontikes [a], D. Koumpouri [b], G.N. Angelopoulos [b,*]

[a] Department of Metallurgy and Materials Engineering, KU Leuven, Kasteelpark Arenberg 44 bus 2450, B-3001 Heverlee, Leuven, Belgium
[b] Laboratory of Materials and Metallurgy, Dept. of Chemical Engineering, University of Patras, 26500 Rio, Greece

ARTICLE INFO

Article history:
Received 29 March 2012
Received in revised form 6 August 2013
Accepted 10 August 2013
Available online 20 August 2013

Keywords:
Calcium ferroaluminate belite clinker
Electric arc furnace steel slag
Cr^{VI}
Hydration
FGD gypsum

ABSTRACT

This study investigated the use of 10 (M1), 17 (M2) and 27 wt.% (M3) electric arc furnace steel slag (EAFS) as a raw material in the production of calcium ferroaluminate belite cement clinker, after firing at 1320 °C. The thermal behavior of the raw meals was studied by TG/DSC and XRD whereas for the analysis of the clinkers, XRD/QXRD, SEM/EDS and EPMA were employed. The resulting clinker was co-grinded with 5 and 20 wt.% Flue Gas Desulfurization (FGD) gypsum and the properties were determined by a series of tests in accordance to EN standards. The evolution of hydration was investigated by SEM and the development of compressive strength. The results revealed that the formed phases in the clinkers were C_2S, C_4AF and $C_4A_3\hat{S}$. The main hydration products were ettringite, AFm and hydrogarnet. The leached Cr^{VI} was below 1 ppm in M3. Compressive strength in cements with 5 wt.% FGD gypsum was (in MPa): 18.3 for M1, 14.3 for M2 and 7.8 for M3 at 28 days, whereas for 20 wt.% FGD gypsum, the values were almost doubled.

1. Introduction

The transition towards resource efficient, low-carbon, closed-loop economies is an urgent necessity as our planet faces unprecedented environmental challenges. In the EU, in particular, the prospect of insufficient and often critical raw materials (metals and minerals) will hamper future economic development and actions are taken to prevent this [1]. With regard to industrial residues, the challenge lies in the development of integrated zero-waste flow sheets, which recover both (critical) metals and incorporate the various residues into building materials or other applications.

Worldwide more than 40% of steel production takes place in electric arc furnace (EAF) [2] and is associated with the generation of 20 Mt electric arc furnace steel slag (EAFS). In Europe, 37% of steel slags were used in cement production and 18.8% for road construction in 2010 [3]. In Greece, cement and steel production is about 6 Mt/y and 3.5 Mt/y respectively while EAFS production is 0.3–0.4 Mt/y; less than 1% is used in cement production and about 55% is used as coarse aggregates for road construction [4]. In general, the heavy metal content in slags (particularly V and Cr) is an issue of concern: Cr^{VI} content, for instance, is limited to 2 ppm in the final product according to the EU Directive 2003 [5].

The past 30 years have seen the emergence of a number of alternative "greener" types of cement. However, in contrast to Portland cement, these new varieties have limited application in mainstream construction. Calcium ferroaluminate (CFAB), or sulfoaluminate belite cements (CSAB) are called "The Third Cement Series" [6,7] and find limited use in China. Ferroaluminate cements contain mainly C_4AF, C_2S, $C_4A_3\hat{S}$, and $C\hat{S}$. As a result, they are able to accommodate high quantities of iron and sulfur, being interground with 16–25 wt.% gypsum [8]. Compared to Ordinary Portland Cement (OPC) which has C_3S as its main compound, these cements require lower clinkering temperatures. Moreover, their clinkers are more friable due to their high porosity resulting also in energy reduction during grinding.

The hydration rate of $C_4A_3\hat{S}$ (Eq. (1)) is very fast, leading to the formation of trisulfoaluminate hydrate ($C_6A\hat{S}_3H_{32}$, AFt) [9]. In the absence of adequate gypsum, $C_4A_3\hat{S}$ reacts only with water (Eq. (2)) and forms monosulfoaluminate hydrate ($C_4A\hat{S}H_{12}$, AFm) [10]. In both cases crystalline $Al(OH)_3$ is also formed.

$$C_4A_3\hat{S} + 2C\hat{S}H_2 + 34H \rightarrow C_6A\hat{S}_3H_{32} + 2AH_3 \quad (1)$$

$$C_4A_3\hat{S} + 18H \rightarrow C_4A\hat{S}H_{12} + 2AH_3 \quad (2)$$

The ferrite phase, with a lack of anhydrite in the mixture, hydrates (Eq. (3)) to form hydrogarnet ($C_3(A_{0.75}F_{0.25})H_6$), whereas if sufficient gypsum is available, ettringite ($C_6A\hat{S}_3H_{32}$) and AFm are formed (Eqs. 4 and 5) [11].

* Corresponding author. Tel.: +30 2610969530; fax: +30 2610990917.
E-mail address: angel@chemeng.upatras.gr (G.N. Angelopoulos).

0958-9465/$ - see front matter © 2013 Elsevier Ltd. All rights reserved.
http://dx.doi.org/10.1016/j.cemconcomp.2013.08.002

$$C_4AF + 10H \rightarrow (4/3)C_3(A_{0.75}F_{0.25})H_6 + (2/3)FH_3 \quad (3)$$

$$C_4AF + 3C\hat{S}H_2 + 30H \rightarrow C_6A\hat{S}_3H_{32} + FH_3 + CH \quad (4)$$

$$C_4AF + C\hat{S}H_2 + (n+2)H \rightarrow C_4A\hat{S}H_n + FH_3 + CH \quad (5)$$

During the hydration of the ferrite phase, the formation of other calcium aluminate phases is also possible, however these are metastable and the formation of hydrogarnet is favored [12]. Due to their low pH, low porosity and the ability of ettringite and AFm phases to bind heavy metals, CSAB–CFAB cements are of interest in hazardous waste encapsulation fields [13–15]. It has been suggested that hydrogarnet can host high quantities of Cr^{VI} [16]. Still, concerns do exist as well: the main hydrating phase, ettringite, is said to be prone to carbonation [17], thus posing a durability question, and they are sometimes expansive.

Recent studies conducted by various researchers show well developed results concerning the incorporation of different wastes as raw materials in CFAB–CSAB cement production. Wu et al. [18] have studied the use of municipal solid waste incineration (MSWI) fly ash in CSAB cements up to 30 wt.% and obtained a cement with high early compressive strength but lower strength gain in later ages. The results also showed that expansive properties are strongly dependent on gypsum content and that all the elements investigated for leaching in the hydrated paste are either well bounded in the clinker minerals or immobilized in the hydration products. Berger et al. [19] studied the potential of CSAB cements with 0 and 20 wt.% gypsum addition for $ZnCl_2$ stabilization/solidification. The use of 20 wt.% gypsum was beneficial in different ways, including improved compressive strength results. Arjunan et al. [20] have successfully prepared CSAB cements with satisfactory compressive strength, using bag house dust, low calcium fly ash and scrubber sludge. By using up to 30 wt.% phosphogypsum in the production of CSAB cements, Peysson et al. [21] concluded that the delayed ettringite precipitation led to a cement paste being damaged by high porosity and consequent cracking. Pelletier-Chaignat et al. [22] observed that at high CSAB/gypsum ratios, gypsum is consumed after 7 days. Luz et al. [23] produced blended cements by mixing 75 wt.% CSAB with 25 wt.% galvanic sludge that delivered acceptable compressive strength and good Cr retention. To the best of our knowledge, only Adolfsson et al. [24] used up to 25 wt.% EAFS as raw material in the production of CFAB type cements, but in combination with other steelmaking slags. This resulted in a cement with low mechanical strength in the later days of hydration.

The present work explores the production of calcium ferroaluminate belite cement clinker with 10 wt.%, 17 wt.% and 27 wt.% EAFS. The central aim was to understand the influence of EAFS on the clinkering process, on the microstructure of clinker and hydration products and on the main properties of the final cement mortars. The role of FGD gypsum co-grinded with the clinker in 5 wt.% and 20 wt.%, in order to control the hydrogarnet formation, was also briefly addressed through compressive strength measurements of hardened mortars.

2. Materials and methods

The raw materials used in the preparation of the raw meals were EAFS, limestone, bauxite and gypsum. EAFS was used as received from SOVEL S.A. industry, Greece. The chemical analysis (Table 1) was performed by XRF (Philips PW 2400). The crystalline phases (Fig. 1) were identified by XRD (SiemensD5000) using DIFFRACplus EVA® software (Bruker-AXS) based on the ICDD Powder Diffraction File. The parameters used were 2θ range of 10–70°, Cu Kα radiation under 40 kV and 30 mA, 0.01° step size and step time of 1°/min. Quantitative determination was performed using the TOPAS® software (Bruker-AXS) based on the Rietveld method, normalized (Table 2). For the estimation of the mineralogical phases of the clinkers, modified Bogue equations were adapted to the thermodynamic system $CaO–SiO_2–Al_2O_3–Fe_2O_3–SO_3$ ($CSAF\hat{S}$) [25–27]. The phases expected to form were C_4AF, C_2S, $C_4A_3\hat{S}$ and $C\hat{S}$. Equations from 6 to 10 were used for the calculations (results are presented in Table 3).

Table 1
Chemical composition of raw materials, wt.%.

Raw materials	EAFS	Limestone	Bauxite	Gypsum
CaO	32.50	48.90	3.62	31.80
FeO_{total}	26.30	1.00	23.00	0.04
SiO_2	18.10	9.00	14.30	1.76
Al_2O_3	13.30	1.36	49.20	0.18
MnO	3.94	n.d.	n.d.	n.d.
MgO	2.53	0.65	n.d.	1.85
Cr_2O_3	1.38	n.d.	n.d.	n.d.
P_2O_5	0.48	n.d.	n.d.	n.d.
TiO_2	0.47	n.d.	2.00	n.d.
SO_3	0.44	n.d.	0.23	41.54
BaO	0.14	n.d.	n.d.	n.d.
Na_2O	0.13	0.10	n.d.	n.d.
K_2O	n.d.	0.15	n.d.	n.d.
V_2O_5	0.06	n.d.	n.d.	n.d.
LOI	<0.50	38.00	10.00	23.14
Total	99.77	99.16	102.35	100.31

LOI: loss on ignition, n.d.: not determined.

$$\%C_4AF = 3.043(\%Fe_2O_3); \quad (6)$$

$$\%C_4A_3\hat{S} = 1.995(\%Al_2O_3) - 1.273(\%Fe_2O_3); \quad (7)$$

$$\%C_2S = 2.867(\%SiO_2); \quad (8)$$

$$\%C\hat{S} = 1.700(\%SO_3) - 0.445(\%Al_2O_3) + 0.284(\%Fe_2O_3); \quad (9)$$

$$\%C = 1.000(\%CaO) - 1.867(\%SiO_2) - 1.054(\%Fe_2O_3) - 0.550(\%Al_2O_3) - 0.700(\%SO_3); \quad (10)$$

The mineralogical phases of the clinkers were calculated also by the Rietveld method (QXRD) using the "Topas® Academic" software, besides the estimations derived from the Bogue equations (Table 3). The quality indexes, lime saturation factor (LSF), silica modulus (SM) and alumina modulus (AM) have been calculated based on established equations [7,28]. The results are presented in Table 3.

The synthesis of the raw meals was calculated by means of an MS Excel© worksheet, by regulating the content of limestone, bauxite and gypsum and by setting the desirable range of variation in the quality indexes LSF, AM and SM. Three types of clinker were prepared with 10 wt.% (M1), 17 wt.% (M2) and 27 wt.% (M3) EAFS content respectively. The content of the raw meals in limestone/bauxite/gypsum/EAFS (in wt.%) was: 62.0/20.0/8.0/10.0 for M1, 61.0/16.0/6.0/17.0 for M2 and 59.5/10.5/3.0/27.0 for M3. A small fluctuation in LSF, AM and SM is present.

For clinker production, all raw materials were individually milled in a Siebtechnik® planetary mill at a particle size <90 μm. After mixing and homogenization with a minimum water addition, pellets of 15–20 mm diameter were created. Dehydration took place in a muffle furnace at 110 °C for 24 h. For clinkering, the pellets were loaded in a magnesia–chrome refractory crucible covered with a lid in order to minimize gas emissions during firing. A Super Kanthal resistance furnace (Nabertherm®) was used. To stabilize the α'- and β-C_2S polymorphic forms, the clinker was cooled fast by the simultaneous application of blown air and crushing by means of a hammer.

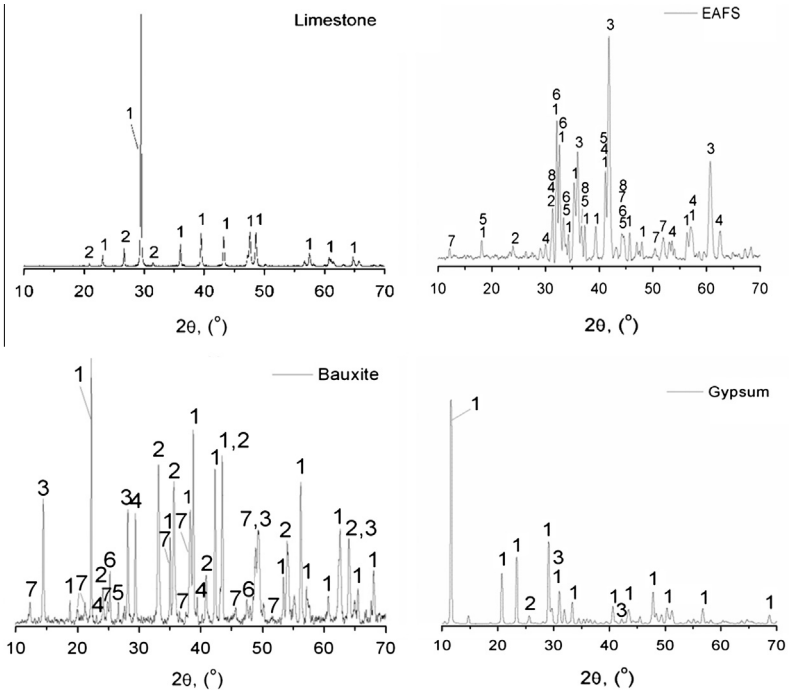

Fig. 1. XRD patterns of the raw materials: (a) limestone: 1 – calcite and 2 – quartz, (b) EAFS: 1 – larnite, 2 – gehlenite, 3 – wüstite, 4 – magnetite, 5 – mayenite, 6 –merwinite, 7 – brownmillerite, 8 - spinel, (c) bauxite: 1 – diaspore, 2 – hematite, 3 – boehmite, 4 – calcite, 5 – quartz, 6 – anatase and 7 – kaolinite and (d) gypsum: 1 – gypsum, 2 – quartz and 3 – dolomite.

Table 2
Mineralogical phase composition of the raw materials, wt.%, according to normalized Rietveld analysis.

EAFS		Limestone		Bauxite		Gypsum	
Larnite	41.0	Calcite	91.1	Diaspore	34.1	Gypsum	91.5
Gehlenite	14.7	Quartz	8.9	Hematite	22.8	Quartz	1.2
Wüstite	12.0			Boehmite	16.5	Dolomite	7.3
Magnetite	10.0			Kaolinite	18.1		
Brownmillerite	9.4			Calcite	5.2		
Mayenite	7.2			Anatase	2.1		
Merwinite	3.7			Quartz	1.2		
Spinel	2.0						
Total	100		100		100		100

Table 3
Estimated (Bogue) and measured (Rietveld-normalized) mineralogical composition, wt.%, of the prepared clinkers and quality indexes results, %.

Clinker type	M1		M2		M3	
	Bogue	Rietveld	Bogue	Rietveld	Bogue	Rietveld
Mineralogical phases, wt.%						
C_2S	42.3	44.6	44.2	43.4	47.0	40.3
C_4AF	33.8	33.0	37.5	38.9	42.6	45.6
$C_4A_3\hat{S}$	19.7	21.5	15	15.6	8.6	11.7
$C\hat{S}$	3.9	0.0	2.9	0.0	1.4	0.0
C	0.3	0.7	0.4	1.6	0.4	1.2
MgO	0.0	0.2	0.0	0.5	0.0	1.2
Total	100	100	100	100	100	100
Quality indexes, %						
LSF	76.12		76.70		77.03	
AM	1.53		1.25		0.95	
SM	0.52		0.56		0.60	

Preliminary investigations on the raw meals were performed by TG–DSC (Netzsch STA 409C) thermal analysis with a 10 °C/min heating rate up to 1350 °C in static air [29] and XRD (2θ range of 10–65°) characterization of M1 pellets after firings at 800 °C, 1000 °C, 1100 °C, 1200 °C, 1270 °C and 1320 °C, with 40 min soaking time. Fast cooling was applied as described above. This approach was followed in order to understand the thermal transformations between 800 °C and 1350 °C, aiming also to select the proper clinkering temperature. The data revealed that at 1270 °C the clinker phases were poorly developed whereas substantial liquid phase formed at 1340 °C (TG–DSC, Fig. 2). At 1320 °C the XRD analysis indicated well crystallized clinker phases, thus firing took place at this temperature. The free lime content after final firing was measured according to ASTM C114-03 and was found consistently below 1 wt.% in all samples.

The final clinkers were analyzed by XRD/QXRD (2θ range of 10–65°) and SEM/EDS (Jeol JSM 6300 and LINK PentaFET 6699, Oxford Instruments, sectioned polished surface, carbon coated). In the case of M1, an electron probe micro-analyzer (EPMA Jeol, JXA-8530F) was employed for the generation of the elemental maps. In order to produce cement, the clinkers were milled in a planetary mill. Flue Gas Desulfurization (FGD) gypsum ($C\hat{S}H_2$), provided by TITAN Cement Company S.A., Greece, was added in 5 wt.% and 20 wt.% in order to control the hydrogarnet formation. As reported elsewhere [30,31], C_4AF reacts with gypsum after 3 days of

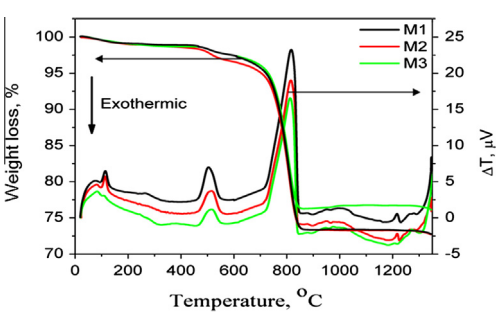

Fig. 2. TG–DSC profiles of the raw meals: M1, M2 and M3.

hydration forming ettringite instead of hydrogarnet, which also improves compressive strength. The low gypsum addition was chosen to obtain a lower weight ratio of $C\hat{S}H_2/C_4A_3\hat{S}$ than the one required by stoichiometry of Eq. (1), whereas the higher one for an excess. This approach was followed in order to understand the role of FGD gypsum on the compressive strength results and hydration products. FGD gypsum was chosen over ordinary one as it proved to be more reactive, in line with results reported elsewhere [32]. Specific surface (Blaine method) was determined according to EN 196-6 [33]. Density was measured by the pycnometer method. Initial setting time, soundness and compressive strength were tested according to EN 196-3 [34] and EN 196-1 [35] respectively. EN 196-10 [36] was used to determine Cr^{VI}.

For the hydration studies, the cements produced were mixed with water at a ratio of 0.5 w/s (water/solid) and the paste was placed in plastic containers. After 1 day, 3 days, 7 days and 28 days of hydration, the process was halted by immersing the pastes in an acetone bath for 2 h followed by drying at 70 °C for 24 h [29]. The hydrated products were analyzed by SEM (gold coated samples).

3. Results and discussion

3.1. Characterization of raw materials

The chemical composition of the raw materials is presented in Table 1, the XRD patterns in Fig. 1 and the quantification by Rietveld method in Table 2. EAFS contains high amounts of CaO, FeO_{total}, SiO_2 and Al_2O_3. The Cr_2O_3 content is 1.38 wt.%; the levels of P_2O_5, TiO_2 and SO_3 are comparable, 0.4–0.5 wt.%. EAFS also contains a small amount of BaO (0.14 wt.%) which may act as a dopant if introduced into the crystal lattice of belite stabilizing the α′- and β-polymorphic forms of C_2S (the α′-form typically being more reactive than the β-form) [37].

The identified phases by X-ray diffraction for limestone are calcite ($CaCO_3$) and quartz (SiO_2), for gypsum are gypsum ($Ca_2SO_4 \cdot 2H_2O$), quartz (SiO_2) and dolomite ($CaMg(CO_3)_2$) and for bauxite are diaspore (α- or β-AlO(OH)), hematite (Fe_2O_3), boehmite (γ-AlO(OH)), calcite ($CaCO_3$), quartz (SiO_2), anatase (TiO_2) and kaolinite ($Al_2Si_2O_5(OH)_4$). EAFS is composed of 41 wt.% larnite (β-Ca_2SiO_4) and 15 wt.% gehlenite ($Ca_2Al(AlSi)O_7$) along with wüstite (FeO), magnetite (Fe_3O_4), brownmillerite ($Ca_2(AlFe_3)_2O_5$), mayenite ($Ca_{12}Al_{14}O_{33}$), merwinite ($(Ca_3Mg(SiO_4)_2$) and spinel ($MgAl_2O_4$). Larnite is stabilized probably due to the combined action of minor additions in the lattice and the fast cooling practice in the slag yard, where water is sprayed over in order toincrease the anti-skid properties when the slag is used as road aggregate.

3.2. Synthesis of raw meals

The estimated (Bogue) phases and quality indexes are presented in Table 3. Increasing the slag causes an increase in LSF to 76.12% for M1, 76.70% for M2 and 77.03% for M3. Due to the low SiO_2 content, SM has values less than 1% which is typical of this type of clinker. AM varies from 1.53% (M1) to 0.95% (M3), due to the low Al_2O_3 content.

3.3. Thermal analysis of raw meals

The TG–DSC results are presented in Fig. 2 whereas Fig. 3 presents the diffraction patterns of M1. The total weight loss is 23.9 wt.%, for M1, 23.2 wt.% for M2 and 22.7 wt.% for M3. Up to 600 °C, the weight loss accompanied by endothermic peaks is due to dehydration (at about 100 °C) and dehydroxylation (at about 450 °C). The decarbonation of calcite and dolomite, indicated by the higher weight loss and the strong endothermic peak, take

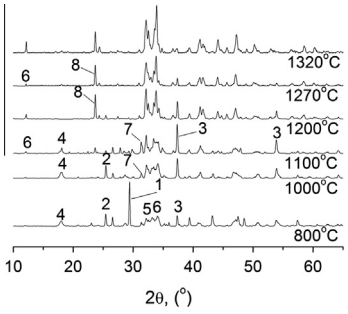

Fig. 3. XRD patterns of M1 at different firing temperatures: 1 – calcite, 2 – anhydrite, 3 – lime, 4 – mayenite, 5 – dicalcium silicate, 6 – tetracalcium alumino ferrite, 7 – calcium silicate sulfate, and 8 – yeelimite.

place in the range of 600–900 °C [7]. A small weight loss above 1200 °C can be attributed to gas emissions of the contained sulfur [31]. At approximately 1200 °C, a small endothermic peak is also present. This peak can be attributed to the dissociation of calcium silicate sulfate compound [6]. Finally, the endothermic peak at about 1340 °C corresponds to melting. The total weight loss decreases as the EAFS content in the raw meal increases, attributed to lower CO_2 emissions in view of the absence of carbonates in EAFS.

The XRD pattern reveals that anhydrite ($CaSO_4$) and calcite ($CaCO_3$) are still present at 800 °C. Calcite decomposes in excess of this temperature and free lime (CaO) is detected. The peak height of anhydrite is reduced over 1100 °C and disappears above 1270 °C. Above 1000 °C, calcium silicate sulfate ($C_5S_2\hat{S}$) is formed. At 1100 °C, yeelimite formation starts and calcium silicate sulfate is still present. At 1180 °C calcium silicate sulfate decomposes to form dicalcium silicate (C_2S) [6] and is no longer present at 1200 °C. Yeelimite was also formed in appreciable amounts as indicated by the increase of its peak intensity [38]. In the temperature range of 800–1100 °C, mayenite ($C_{12}A_7$) is present, presumably originating in part from the slag, while the remainder is formed from the reaction of the other raw materials as expected for clinkers with LSF in the range of 75% [6]. Above 1100 °C mayenite reacts presumably with the other constituents in the matrix towards tetracalcium alumino ferrite (C_4AF) and yeelimite ($C_4A_3\hat{S}$). Indeed, the three major phases in the clinkers, namely C_2S, C_4AF and $C_4A_3\hat{S}$ are well crystallized above 1270 °C as indicated by the comparatively higher peak intensities. The aforementioned sequence of reactions concurs with those reported by Lawrence [6].

3.4. Mineralogy of the clinkers

The XRD patterns of M1, M2 and M3 clinkers are presented in Fig. 4, whereas the quantification by Rietveld method, in Table 3. In all clinkers the characteristic peaks of tetracalcium alumino ferrite (C_4AF), larnite (β-C_2S) and yeelimite ($C_4A_3\hat{S}$) are identified. The peak intensity of yeelimite decreases as the slag content in the raw meal increases. The $C\hat{S}$ was not detected, probably due its very low content as it either reacts or was emitted as sulfur.

A slight difference between measured Rietveld and estimated Bogue method is observed, especially in the case of M1 and M2. The findings are in agreement with other works [31], indicating that adapted Bogue equations can be used to predict the mineralogical phases in this type of clinker. Concerning Rietveld calculations, increasing the slag content is decreasing the content of C_2S phase, varying from 44.6 wt.% (M1) to 40.3 wt.% (M3), whereas for the C_4AF and $C_4A_3\hat{S}$ phases holds the opposite. Values varied from 33 wt.% (M1) to 45.6 wt.% (M3) for C_4AF and 21.5 wt.%

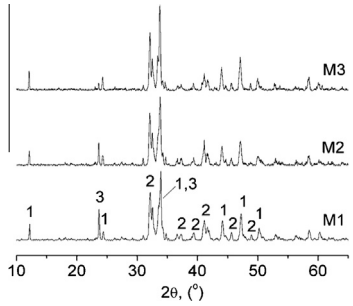

Fig. 4. XRD patterns of M1, M2 and M3 clinkers. The main minerals are: 1 – tetracalcium alumino ferrite, 2 – larnite and 3 – yeelimite.

(M1) to 11.7 wt.% (M3) for $C_4A_3\hat{S}$. $C\hat{S}$ was not found in any of the mixtures, indicating that probably a part dissociated or reacted towards the formation of $C_4A_3\hat{S}$ phase. This could explain the difference between Rietveld and Bogue results of these two phases. A small increment of free lime (C) above 1 wt.% was found in the case of M2 and M3, whereas of MgO only in M3. These type of cement systems (CSAF$\hat{S}$) were found to be able to accommodate up to 10 wt.% MgO [6] without an expansive behavior.

3.5. Microstructure and microchemistry of the clinkers

Backscattered electron images (BEI) on an EDS spectrum from the microanalysis of the different phases are presented in Fig. 5 whereas a WDS elemental mapping of M1 in Fig. 6. The BEI reveal the formation of the yeelimite ($C_4A_3\hat{S}$), tetracalcium alumino ferrite (C_4AF) and dicalcium silicate (C_2S) phases in differing intensities of grey. In all cases porosity is observed, which is typical for CFAB cements [31]. Rounded belite grains are also visible in the pores.

From WDS elemental mapping the presence of yeelimite, tetracalcium alumino ferrite and dicalcium silicate phases are confirmed. The dark grey areas consist of Al in high levels, and Ca and S in lower levels. Low amounts of Fe have been found also. These areas derive from yeelimite phase formation, being reported [31,38] as able to intake distinct amounts of Fe in its crystalline lattice. The lighter grey areas contain high levels of Ca and low levels of Si. In these areas referred here as dicalcium silicate phases, traces or no Al, Fe and S are found. The light grey areas consist of the interstitial phase and tetracalcium alumino ferrite is dominant with Ca from moderate to high level, Al from low to medium level and Fe from moderate to high level. Low or no S and Si content are found in these areas.

3.6. Density and grindability of the cement

The density values presented increase with increasing EAFS content: 2.9 g/cm^3 for M1, 3.1 g/cm^3 for M2 and 3.3 g/cm^3 for M3. In order to obtain Blaine finenesses of 4100 ± 20 cm^2/g, the required milling time was 73 s for M1, 85 s for M2 and 89 s for M3. The above results indicate that increasing slag content leads to a less grindable clinker, most probably due to the increment of C_4AF [39].

3.7. Physical properties of the cement paste and Cr^{VI} content

Table 4 presents the results of water demand, initial setting time and soundness. Increasing the slag addition increases the setting time as a result of lower ettringite formation. In all three cases the initial setting time values were below EN 197-1 standard requirements. Soundness did not exceed 1 mm, indicating that the ettringite expansion was not extended despite theobserved speed of setting (fast).

Cr^{VI} was measured only in M3 and was below 1 ppm. For M1 and M2, the faster setting time did not allow obtaining the minimum amount of filtrate required for analysis and therefore Cr^{VI} determination was not feasible. However it is expected that Cr^{VI} would be lower than the value for M3 (<1 ppm) due to the lower slag content in these cements (as slag is the main carrier for Cr).

3.8. SEM analysis of the hydration products

Secondary electron images (SEI) of M1, M2 and M3 hydrated pastes for 1 day, 3 days, 7 days and 28 days are presented in Fig. 7. Yeelimite reacted very fast with water and FGD gypsum, presenting ettringite-like needles after only 1 day in all cement pastes. From 3 days and beyond, AFm flakes and round, smooth, small crystals of hydrogarnet [40] are formed. In all three mixtures

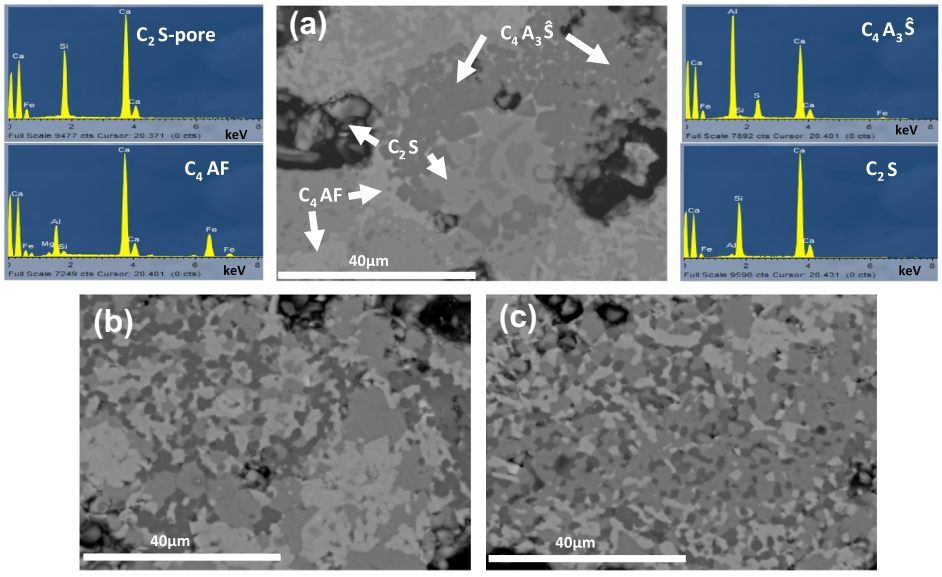

Fig. 5. BEI on polished section of the produced clinkers: (a) M1, (b) M2 and (c) M3. Minerals identified are: yeelimite ($C_4A_3\hat{S}$), dicalcium silicate (C_2S) and tetracalcium alumino ferrite (C_4AF).

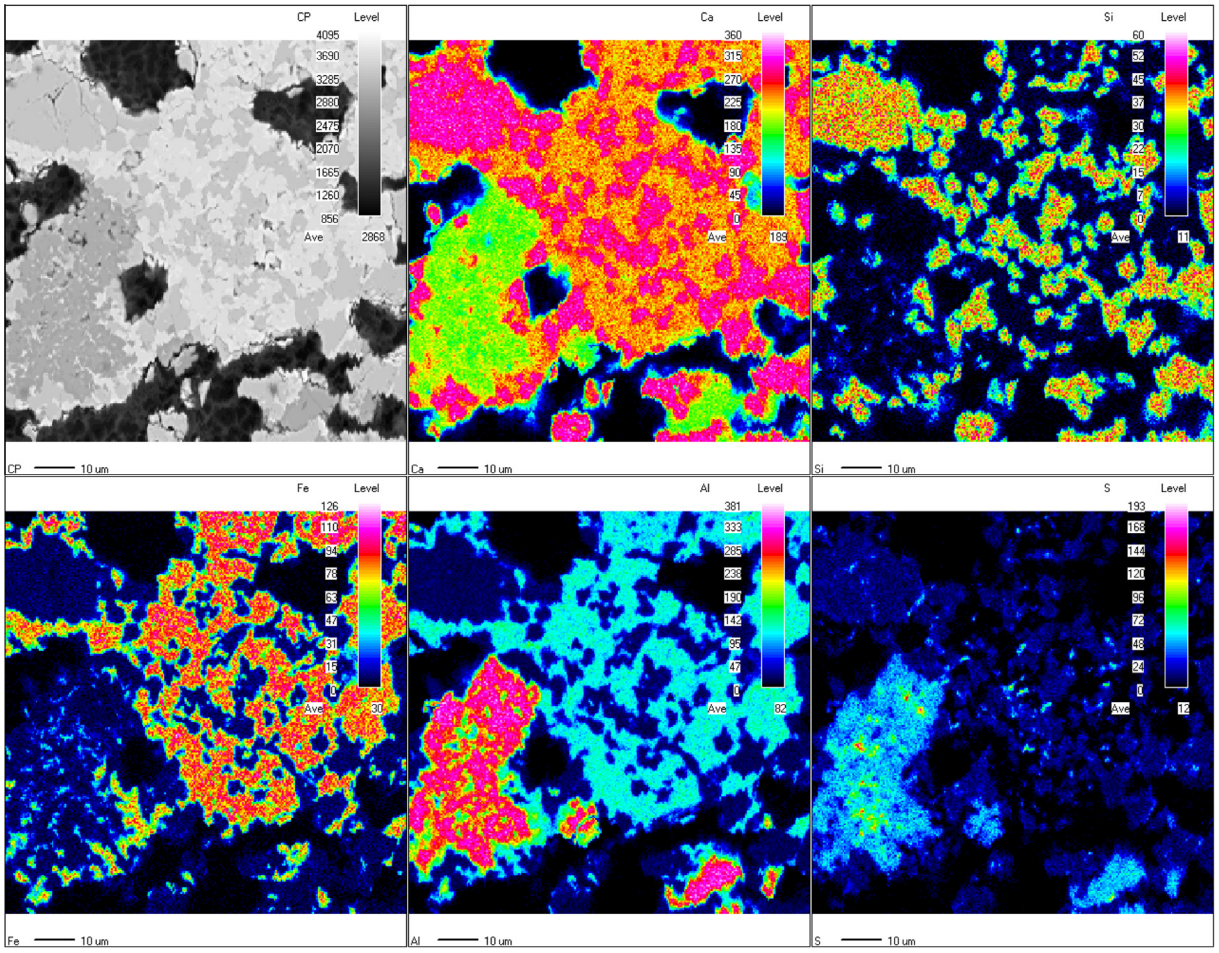

Fig. 6. WDS elemental mapping of M1. Left to right, top row: CP (Backscattered electron image of analyzed area), Ca and Si; second row: Fe, Al and S.

Table 4
Results of water demand, initial setting time and soundness of the cement pastes.

Cement type	Water demand (wt.%)	Initial setting time (min.)	Soundness (mm)
M1	45.0	7	0.9
M2	37.5	12	0.7
M3	35.0	15	0.7

due to the lower weight ratio of $C\hat{S}H_2/C_4A_3\hat{S}$ than the one required by stoichiometry of Eq. (1), taking into consideration Rietveld results, the remaining $C_4A_3\hat{S}$ reacted to form AFm flakes in lack of gypsum. Hydrogarnet is also visible from the reaction of C_4AF with water in lack of gypsum. In M3 the formation of hydrogarnet was relatively extended as a result of the increased slag content.

3.9. Compressive strength

The compressive strength results for 5 wt.% and 20 wt.% FGD gypsum addition are presented in Fig. 8. It was observed that increasing slag content in the raw meal corresponds with a decrease in compressive strength due to the reduced $C_4A_3\hat{S}$ and the increased C_4AF. In M1, M2 and M3, where there was 5 wt.% added gypsum, the compressive strength at 3 days is 13.1 MPa, 10.7 MPa and 6.2 MPa respectively. At 28 days the developed strength is 18.3 MPa for M1, 14.3 MPa for M2 and 7.8 MPa for M3. The observed rather slow increment of strength with time was also found by Lawrence [6] and Adolfsson et al. [6,41] in their studies and therefore these cements are described as slow hardening. The higher early strength of M1 and M2 compared with M3 is attributed to the higher yeelimite content which reacts with gypsum and water to form ettringite and AFm [42]. Indeed, ettringite forms rapidly and within 1 day develops 70–85% of its final values [43]. With the addition of 5 wt.% FGD gypsum, the weight ratio of $C\hat{S}H_2/C_4A_3\hat{S}$ is low. A low $C\hat{S}H_2/C_4A_3\hat{S}$ ratio results in the formation of ettringite and AFm (from $C_4A_3\hat{S}$) and hydrogarnet (from C_4AF). With a 20 wt.% FGD gypsum addition, the compressive strength results are almost doubled from 3 days of hydration and above. As the results of 1 day are almost identical with those of 5 wt.% FGD gypsum, attributed to the reaction of Klein compound with gypsum in the same extent, the development of strength from 3 days and above can be attributed to the reaction of C_4AF with the remaining gypsum which leads to the formation of ettringite instead of hydrogarnet formation. As the $C\hat{S}H_2/C_4A_3\hat{S}$ weight ratio in this case is higher, these findings are in agreement with other studies [30,31]. Further reports, now under investigation, will provide more data regarding the physical properties and hydration products of this type of clinker with 20 wt.% FGD gypsum content.

4. Conclusions

- The production of calcium ferroaluminate belite cements is possible by combining limestone, bauxite and gypsum raw materials together with 10 wt.% (M1), 17 wt.% (M2) and 27 wt.% (M3) EAFS at a firing temperature of 1320 °C.

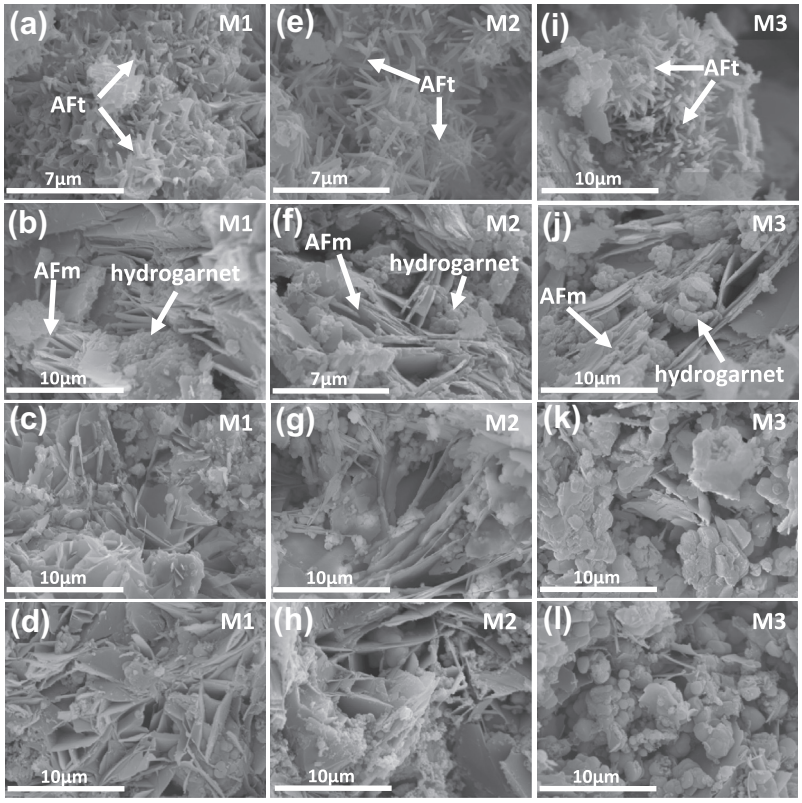

Fig. 7. SEI of the hydrated pastes after different curing periods: M1–1 day (a), 3 days (b), 7 days (c) and 28 days (d), M2 – 1 day (e), 3 days (f), 7 days (g) and 28 days (h), M3 – 1 day (i), 3 days (j), 7 days (k) and 28 days (l).

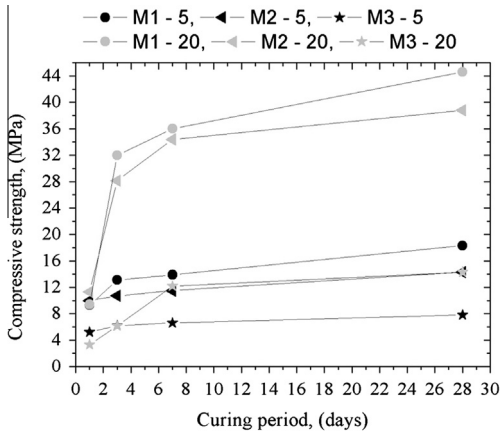

Fig. 8. Compressive strength results of the cement paste after different curing time and wt.% of FGD gypsum retarder (black – 5 wt.%, light grey – 20 wt.%).

- The microstructure of all clinkers constitutes from C_4AF, C_2S and $C_4A_3\hat{S}$; for an increasing slag content, C_4AF and $C_4A_3\hat{S}$ are increasing whereas C_2S is decreasing.
- Increasing the slag addition increases the setting time as a result of lower ettringite formation.
- Soundness did not exceed 1 mm, indicating that ettringite expansion was not extended despite the fast setting observed. Cr^{VI} was found below 1 ppm in M3.
- Mechanical properties are decreased by the slag increment due to the decrease of the $C_4A_3\hat{S}/C_4AF$ ratio and the non-adequate reactivity of belites and ferrites.
- Increasing the quantity of FGD gypsum in cements improves the compressive strength, provided by the high content of C_4AF which probably reacts with the available gypsum to form ettringite instead of hydrogarnet.
- The use of EAFS provides on one hand the advantage of decreasing the CO_2 emissions due to the content in CaO free of CO_2 and on the other hand contributes in saving natural resources (i.e. limestone and clays) due to the relatively high content in oxides such as SiO_2 and Al_2O_3. Moreover, the use of EAFS could also reduce the energy required during clinkering due to less $CaCO_3$ dissociating. A quantity of around 10–17 wt.% could be used, providing acceptable mechanical properties in the presence of gypsum.

Acknowledgments

D. Koumpouri and G.N. Angelopoulos acknowledge the support of the University of Patras through the "Karatheodoris" 2011 research program. Y. Pontikes is thankful to the Research Foundation – Flanders for the post-doctoral fellowship. TITAN Cement Company S.A. and SOVEL S.A. metallurgy industries are gratefully acknowledged for providing the raw materials as well as their technical assistance. The EPMA-WDS work has been feasible due to the support of the Hercules Foundation (Project ZW09-09).

References

[1] European Commission. Critical raw materials for the EU; 2010.
[2] International Iron and Steel Institute. IISI steel statistical yearbook. Belgium Brussels; 2004.
[3] European slag association use of slags in Europe; 2010.
[4] www.aeiforos.gr. [accessed 31.07.12].

[5] European Parliament Directive. 2003/53/EC of the European Parliament and of the Council; 2003.
[6] Lawrence CD. The production of low-energy cements. Lea's chemistry of cement and concrete. 4th ed. Oxford: Butterworth-Heinemann; 2003.
[7] Bhatty JI. Miller FM. Kosmatka, SH: Innovations in Portland Cement Manufacturing Portland Cement Association; 2004.
[8] Glasser FP, Zhang L. High-performance cement matrices based on calcium sulfoaluminate-belite compositions. Cem Concr Res 2001;31(12):1881–6.
[9] Kasselouri V, Tsakiridis P, Malami C, Georgali B, Alexandridou C. A study on the hydration products of a non-expansive sulfoaluminate cement. Cem Concr Res 1995;25(8):1726–36.
[10] Martin D, Martin P, Ladimir K. Heat evolution and mechanism of hydration in $CaO–Al_2O_3–SO_3$ system. Ceram Silikáty 2005;49:104–8.
[11] Nicola M, Christopher H, Andrew CJ, Sally LC, Simon DMJ, Paul B, et al. The paste hydration of brownmillerite with and without gypsum: a time resolved synchrotron diffraction study at 30, 70, 100 and 150° C. J Mater Chem 2004;14:428–35.
[12] Chrysochoou M, Dermatas D. Evaluation of ettringite and hydrocalumite formation for heavy metal immobilization: literature review and experimental study. J Hazard Mater 2006;136(1):20–33.
[13] Albino V, Cioffi R, Marroccoli M, Santoro L. Potential application of ettringite generating systems for hazardous waste stabilization. J Hazard Mater 1996;51(1–3):241–52.
[14] Peysson S, Péra J, Chabannet M. Immobilization of heavy metals by calcium sulfoaluminate cement. Cem Concr Res 2005;35(12):2261–70.
[15] Zhou Q, Milestone NB, Hayes M. An alternative to Portland cement for waste encapsulation–the calcium sulfoaluminate cement system. J Hazard Mater 2006;136(1):120–9.
[16] Hillier S, Lumsdon DG, Brydson R, Paterson E. Hydrogarnet: a host phase for Cr(VI) in chromite ore processing residue (COPR) and other high pH wastes. Environ Sci Technol 2007;41:1921–7.
[17] Zhou Q, Glasser FP. Kinetics and mechanism of the carbonation of ettringite. Adv Chem Res 2000;12(3):131–6.
[18] Wu K, Shi H, Guo X. Utilization of municipal solid waste incineration fly ash for sulfoaluminate cement clinker production. Waste Manage (Oxford) 2011;31(9–10):2001–8.
[19] Berger S, Cau Dit Coumes C, Le Bescop P, Damidot D. Stabilization of $ZnCl_2$-containing wastes using calcium sulfoaluminate cement: cement hydration, strength development and volume stability. J Hazard Mater 194(0):256–67.
[20] Arjunan P, Silsbee MR, Della MR. Sulfoaluminate-belite cement from low-calcium fly ash and sulfur-rich and other industrial by-products. Cem Concr Res 1999;29(8):1305–11.
[21] Peysson S, Pera J, Chabannet M. Immobilization of heavy metals by calcium sulfoaluminate cement. Cem Concr Res 2005;35(12):2261–70.
[22] Pelletier-Chaignat L, Winnefeld F, Lothenbach B, Müler CJ. Beneficial use of limestone filler with calcium sulphoaluminate cement. Constr Build Mater 2012;26(1):619–27.
[23] Luz CA, Rocha JC, Cheriaf M, Pera J. Valorization of galvanic sludge in sulfoaluminate cement. Constr Build Mater 2009;23(2):595–601.
[24] Adolfsson D, Menad N, Viggh E, Björkman B. Hydraulic properties of sulphoaluminate belite cement based on steelmaking slags. Adv Cem Res 2007;19:133–8.
[25] Metha P P. World Cem Technol 1980;11:167.
[26] Sharp J, Lawrence C, Yang R. Adv Cem Res 1999;11:3.
[27] Majling J, Sahu S, Vlna M, Roy D. Cem Concr Res 1993;23:1351.
[28] Nicholas BW. Understanding Cement. United Kingdom: WHD Microanalysis Consultant Ltd.; 2010.
[29] Taylor HFW. Cement chemistry. London: Academic Press; 1990.
[30] Tristana D, Reobert FR, Kevin RH, Robert BJ. Low-energy, low CO_2-emitting cements produced from coal combustion by-products and red mud. In: World of Coal Ash Conference; 2009.
[31] Chen I, Juenger M. Synthesis and hydration of calcium sulfoaluminate-belite cements with varied phase compositions. J Mater Sci 2010;46(8):2568–77.
[32] Tzouvalas G, Rantis G, Tsimas S. Alternative calcium-sulfate-bearing materials as cement retarders: Part II. FGD gypsum Cem Concr Res 2004;34(11):2119–25.
[33] European Committee for Standardization. EN 196-6. Methods of testing cement. Determination of finenesse; 1989.
[34] European Committee for Standardization. EN 196-3. Methods of testing cement – Part 3: determination of setting time and soundness; 1994.
[35] European Committee for Standardization. EN 196-1. Methods of testing cement – Part 1: determination of strength; 1994.
[36] European Committee for Standardization. EN 196-10. Methode of testing cement – Part 10: determination of the water-soluble chromium (VI) content of cement; 2006.
[37] Ghosh SN, Rao BP, Paul AK, Raina K. The chemistry of dicalcium silicate mineral. J Mater Sci 1979;14:1554–6.
[38] Muntean IM, Paul FG, Novac C. Sintering conditions and hydraulic activity of $4CaO·3Al_2O_3·SO_3$. In: Stojanovic BD, Skorokhod VV, Nikolic MV, editors. Advanced Science and Tehnology of Sintering. New York: Kluwer Academic/Plenum; 1999.
[39] Hewlett PC. LEA'S chemistry of cement and concrete, 4th ed.. Elsevier Science & Technology Books; 1998.
[40] Fujita S, Suzuki K, Shibasaki Y, Mori T. Synthesis of hydrogarnet from molten slag and its hydrogen chloride fixation performance at high temperature. J Mater Cycles Waste Manage 2002;4(1):70–6.
[41] Adolfsson D. Steelmaking slags as raw materials for sulphoaluminate belite cement. Sweden: Lulea University of Tehnology; 2006.
[42] Hanic F, Kaprálik I, Gabrisová A. Mechanism of hydration reactions in the system $C_4A_3S–CS–CaO–H_2O$ referred to hydration of sulphoaluminate cements. Cem Concr Res 1989;19(5):671–82.
[43] Beretka J, Marroccoli M, Sherman N, Valenti GL. The influence of C_4A_3S content and WS ratio on the performance of calcium sulfoaluminate-based cements. Cem Concr Res 1996;26(11):1673–81.